Универзитет у Београду
ГЕОГРАФСКИ
ФАКУЛТЕТ

GIS-based methods of past dunes trajectories on satellite images from 2010-2020

[1,2,3] Aleksandar Valjarević
[1]University of Belgrade, Faculty of Geography, Studentski Trg 3/III, 11000 Belgrade, Serbia, e-mail: aleksandar.valjarevic@gef.bg.ac.rs
[2]King Fahd University of Petroleum and Minerals (KFUPM), 31261, Saudi Arabia
[3]Department for Management of Science and Technology Development, Ton Duc Thang University, Ho Chi Minh City, Vietnam
Faculty of Environment and Labor Safety, Ton Duc Thang University, Ho Chi Minh City, Vietnam

Facts about planet and climate

- **Mars is the fourth planet from the sun. The surface of Mars is orange-red in colour as it is covered in iron(III) oxide dust, which has earned it the nickname "Red Planet".**
- **Of all the planets in the solar system, the seasons on Mars are the most Earth-like, due to the similar inclination of the rotational axes of the two planets. The seasons on Mars are about twice as long as on Earth, as Mars' greater distance from the sun means that the Martian year is about two Earth years long. Temperatures on the surface of Mars fluctuate between lows of around −110 °C and highs of up to 35 °C in the equatorial summer.**

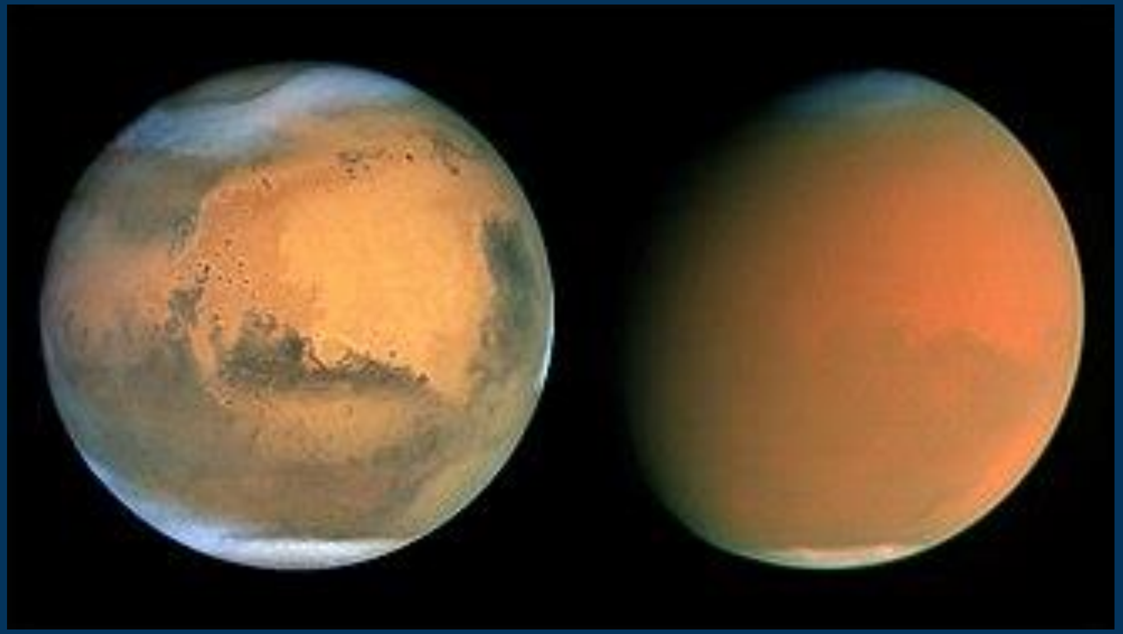

Introduction

The geological time scale on the Mars

- On Mars?

- Pre-Noachian
- Noachian
- Hesperian
- Amazonian

The space missions for the analyses of the planet Mars

Satellite images from the Mars Global Surveyor (1996), Mars Pathfinder (1996), Mars Odyssey (2001), Rosetta (2004), Mars Orbiter Mission (2013), ExoMars Trace Gas Orbiter (2016), InSight (2018), Emirates Mars Mission (2020), Tianwen-1 (2020).

These missions increased quality of images taken from the Mars. These satellite images were in the various resolution.
The resolution are between 10 km^2 an 100 km^2.

Another valuable data used in this research was from the The Mars Orbiter Laser Altimeter (MOLA) and the Mars Express High Resolution Stereo Camera (HRSC) provided very precise results on all aspects of the Martian terrain.

At the end the two types of data were used. In these database iit was useful to find vector and raster data. United States Geological Survey (USGS) , https://www.usgs.gov/ and National Aeronautics and Space Administration (NASA- Map a Planet 2),
https://astrogeology.usgs.gov/search/results?q=MAP2&k1=target&v1=Mars

The differences between vector and raster data

Vector data offers a way to visualise features of the real world in the GIS environment. A feature is anything you can see in the landscape. Imagine you are standing on the top of a hill. When you look down, you see houses, roads, trees, rivers and so on. Each of these things would be a feature if we represented them in a GIS application. Vector features have attributes that consist of text or numeric information describing the features

In its simplest form, a raster consists of a matrix of cells (or pixels) arranged in rows and columns (or a grid), with each cell containing a value representing information such as temperature. Rasters are digital aerial photographs, images from satellites, digital images or even scanned maps.

The differences between vector and raster data

Vector data are useful for analyses of data that have a vector direction and coordinates. In the case of the Martian dunes, all features from the last twenty years of imagination were used and estimated.

Mars is analysed with the help of raster data. The raster data represent the entire area of Mars.

As the satellite images of Mars are not sufficiently suitable for this study, advanced GIS methods were also used.

What does GIS mean?
Geographic information systems are a powerful tool for analysing spatial properties and relationships.

The first look of the problem

Mission and data from the Mars

- The ExoMars Trace Gas Orbiter (TGO), the Emirates Mars Mission (EMM) and possible future stationary Mars satellites will provide innovative data products on the optical depth of dust and water ice clouds in the Martian atmosphere with a temporal resolution of hours. As already mentioned, the data from the MARS, Digital Elevation Model and colour satellite images are not sufficient to fully analyse the characteristics of the dunes and the former pathways.
- Can we observe dune activity lately, do we sometimes have devil's dust winds?

Digitisation of recent geological units on Mars

Some crustal materials on Mars are similar in their silicon content to the continental crust on Earth. In addition, the rounded pebbles and the possible conglomerate as well as the abundant sand- and dust-sized particles speak in favour of a planet that was once rich in water. The strong winds on the planet Mars were in the geological past between 100,000,000 and 200,000,000 years ago.

Fig. 1, added by the author, shows the most important geological features on Mars.

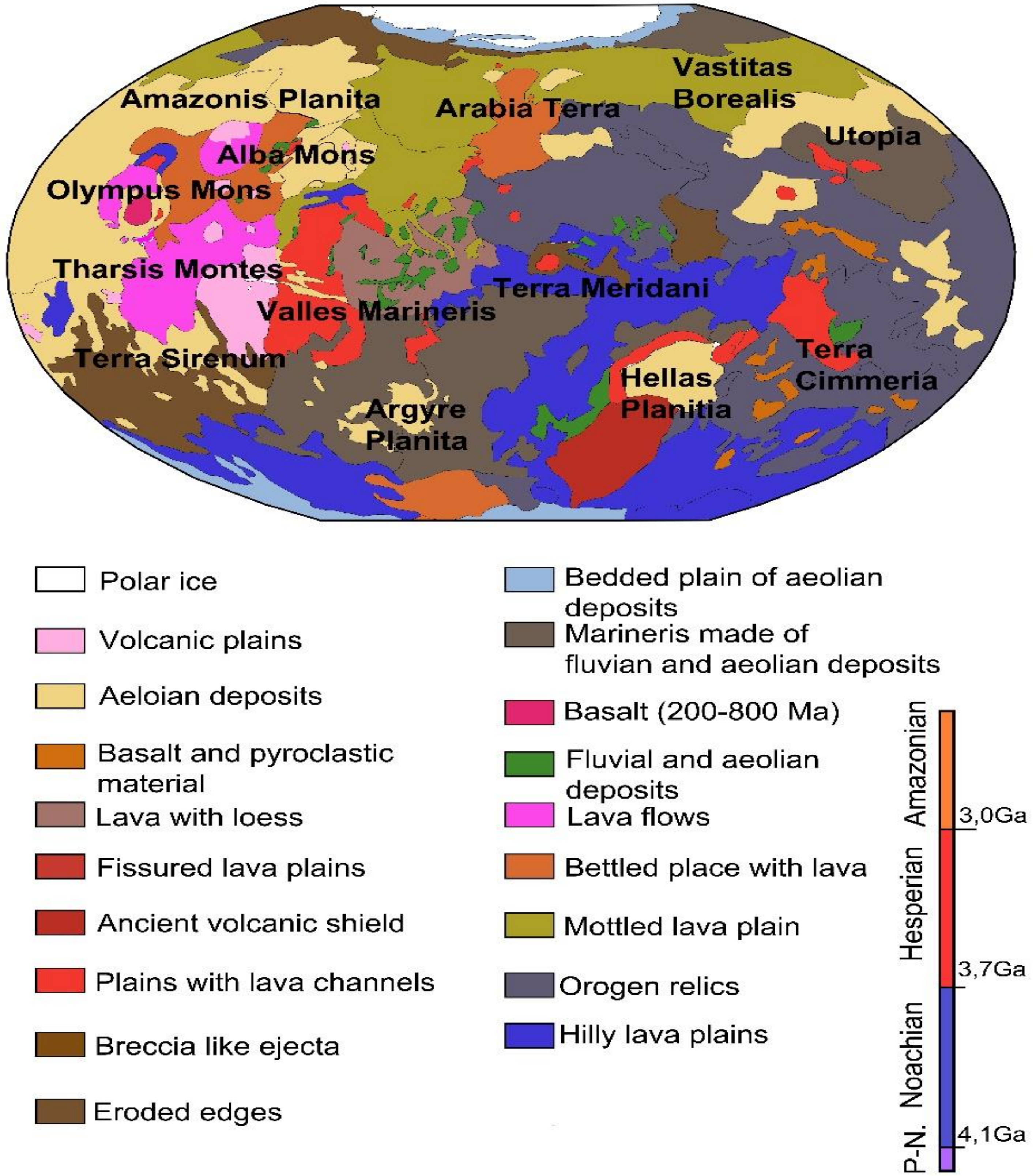

The methods of satellite positioning can be applied part one?

Supervised image classification is based on the creation of algorithms known as training networks. The main methods related to this method are training pixels and known pixels called training pixels. The last phase is the classification phase. All pixels are categorised. The last stage is the output stage.

Unsupervised image classification is associated with algorithms that can analyse unknown pixels. The classification is confirmed by the spectral differences.

The example of NDVI index applied on the Earth ?

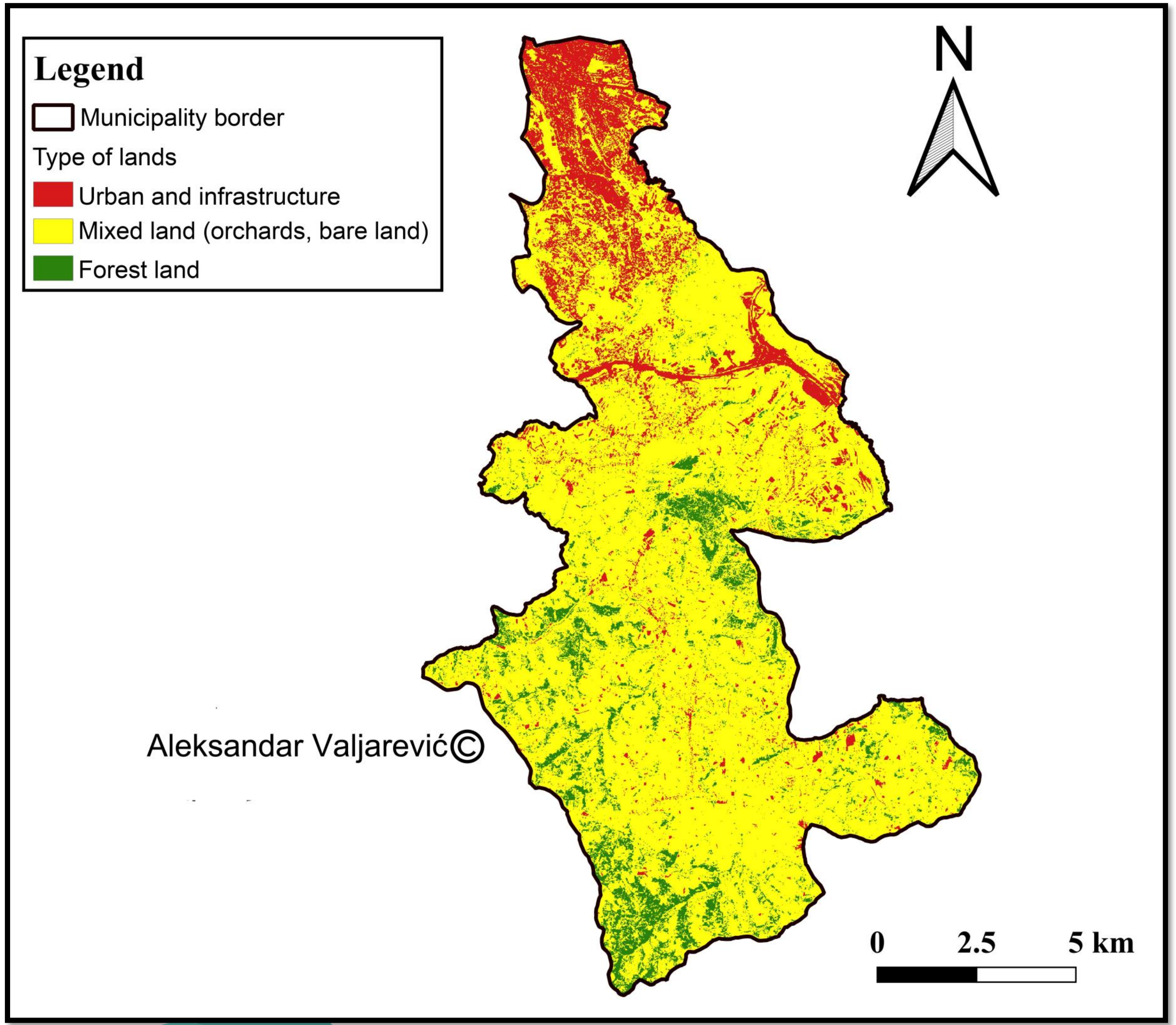

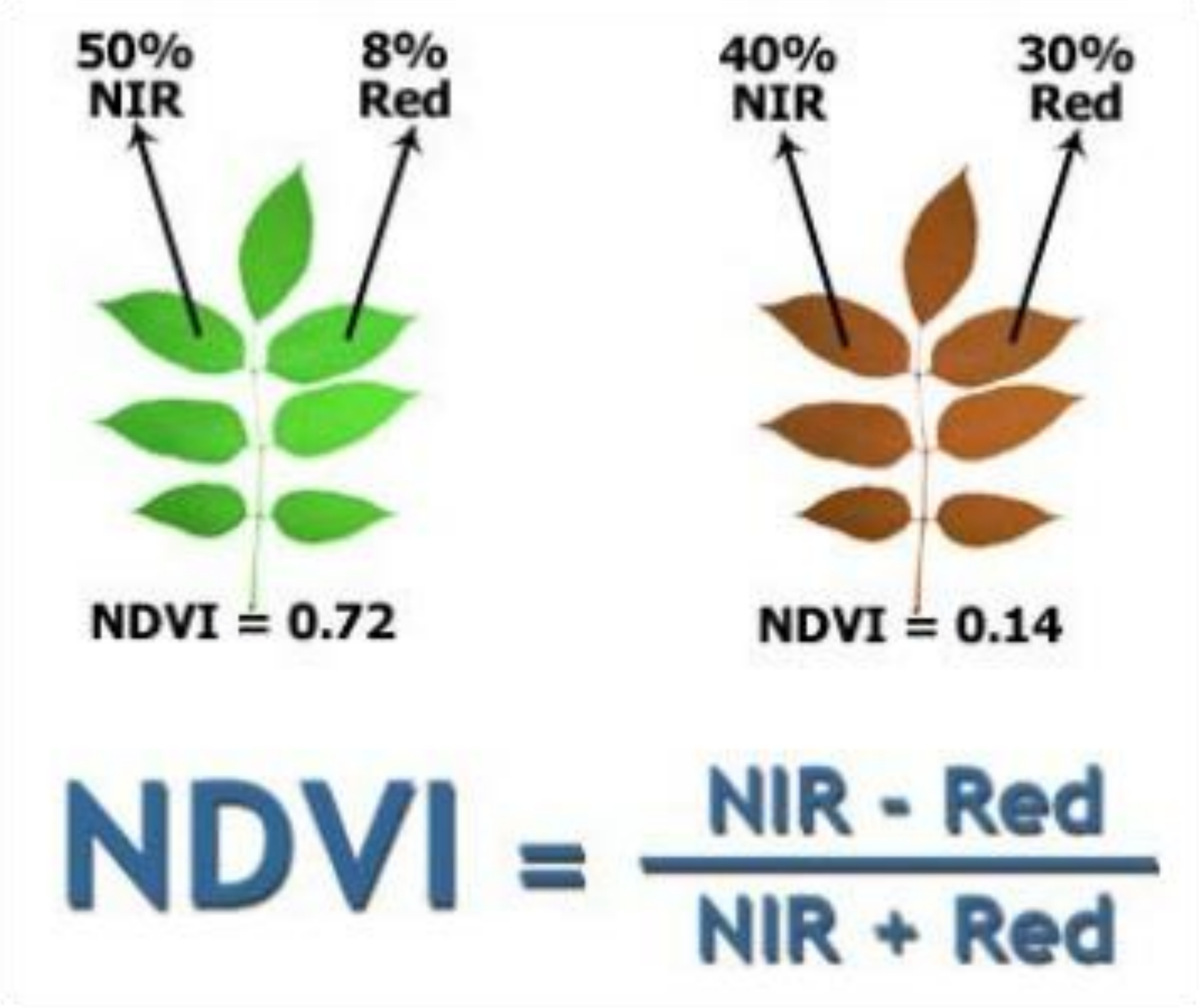

The methods of satellite detection can be applied part two?

Normalized Difference Vegetation Index (NDVI) is used to quantify vegetation greenness and is useful in understanding vegetation density and assessing changes in plant health. The index is easy to interpret: NDVI will be a value between -1 and 1. An area with nothing growing in it will have an NDVI of zero. NDVI is calculated with the following expression: NDVI = (NIR-Red) / (NIR+Red), where NIR is near-infrared light and Red is visible red light.

Very small values (0.1 or less) of the NDVI function correspond to empty areas of rocks, sand or snow.

Moderate values (from 0.2 to 0.3) represent shrubs and meadows, while large values (from 0.6 to 0.8) indicate temperate and tropical forests. The NDVI index is not useful because is not known vegetation of the planet.

The methods of satellite detection can be applied part three?

Normalized Difference Water Index (NDWI) 0,2 – 1 – Water surface, 0.0 – 0,2 – Flooding, humidity, -0,3 – 0.0 – Moderate drought, non-aqueous surfaces, -1 – -0.3 – Drought, non-aqueous surfaces. Of course this index is not useful too, because there is not permanent running water on the Mars, only in micro-freezing stage.

Normalized Difference Snow Index (NDSI) A pixel with NDSI <= 0.0 is a snow free land surface. This index is some way is useful in analyses on the Planet surafce. The values on the North Martian pole *Planum Boreum* (north) varied btween -0.1 to 0.0. The values on the South pole *Planum Australe* (south) varied between -0.1 and -0.2.

The methods of satellite detection can be applied part three?

Normalized Difference Water Index (NDWI) 0,2 – 1 – Water surface, 0.0 – 0,2 – Flooding, humidity, -0,3 – 0.0 – Moderate drought, non-aqueous surfaces, -1 – -0.3 – Drought, non-aqueous surfaces. Of course this index is not useful too, because there is not permanent running water on the Mars, only in micro-freezing stage.

Normalized Difference Snow Index (NDSI) A pixel with NDSI <= 0.0 is a snow free land surface. This index is some way is useful in analyses on the Planet surafce. The values on the North Martian pole *Planum Boreum* (north) varied btween -0.1 to 0.0. The values on the South pole *Planum Australe* (south) varied between -0.1 and -0.2.

The examples of NDWI and NDSI indexes ?

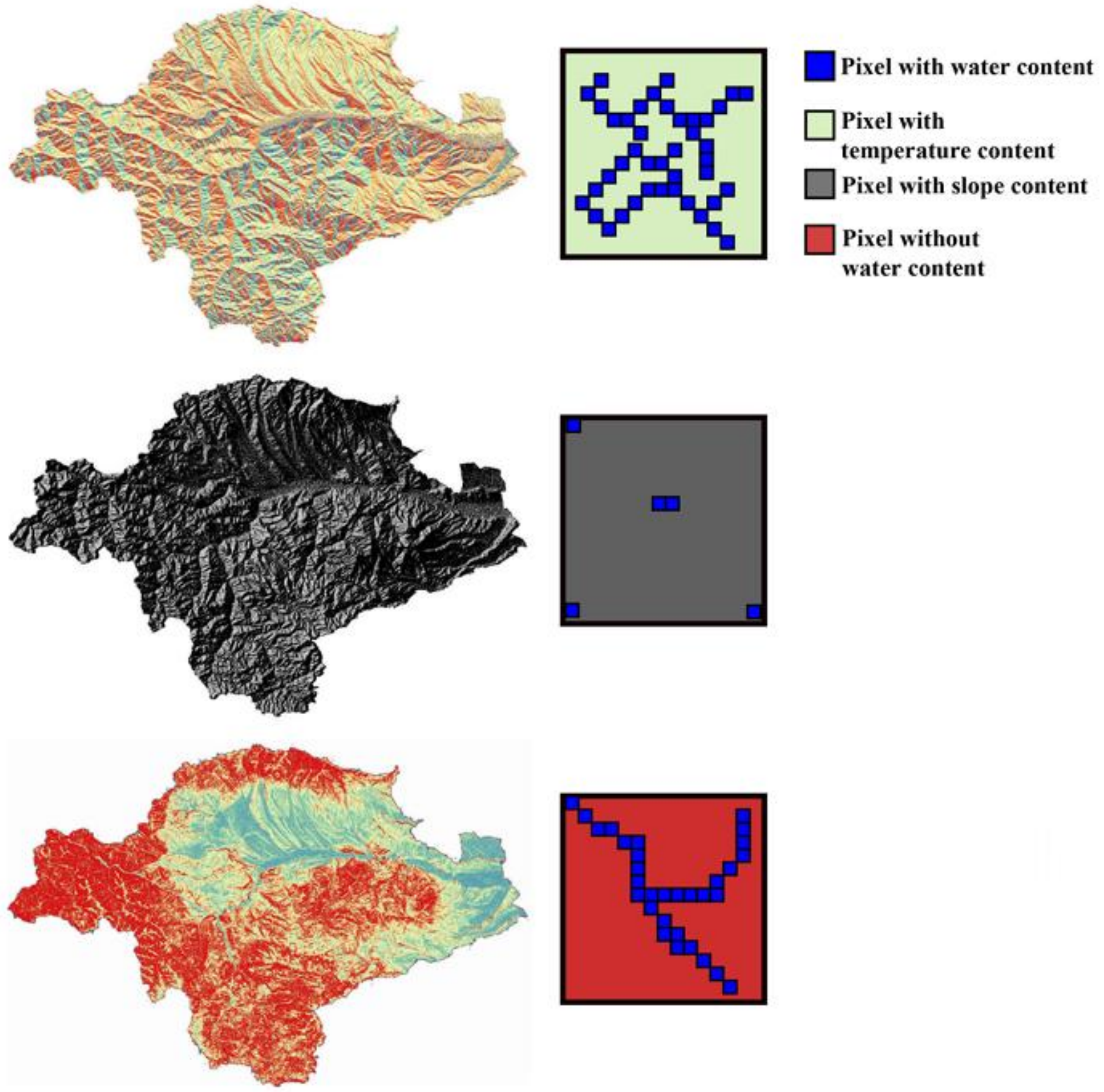

FIGURE 1 Three sub-numerical methods for dew volume calculations

Received: 9 March 2020 | Revised: 22 April 2020 | Accepted: 26 May 2020
DOI: 10.1002/met.1930

RESEARCH ARTICLE

Meteorological Applications RMetS

GIS and remote sensing techniques for the estimation of dew volume in the Republic of Serbia

Aleksandar Valjarević[1,2] | Dejan Filipović[3] | Dragana Valjarević[4] | Miško Milanović[3] | Slaviša Milošević[5] | Nebojša Živić[5] | Tin Lukić[6]

The methods of satellite detection can be applied part three?

Pixel and swapping pixel methods. To determine the dune density and the number of dunes from the Mars images, we used pixel and sub-pixel swapping methods. These methods were introduced to determine the fine resolution of the raster maps.

The linearised pixel swapping method is well suited for the analysis of cadastral parcels. In the standard pixel swapping method, the same exponential distance window is used for each pixel. In the "linearised" version, a unique anisotropic exponential distance decay window is created for each pixel based on the measured anisotropy within the class shares. This biases the sub-pixel swapping to increase the probability of predicting linear features.

The pixel and swaping pixel methods

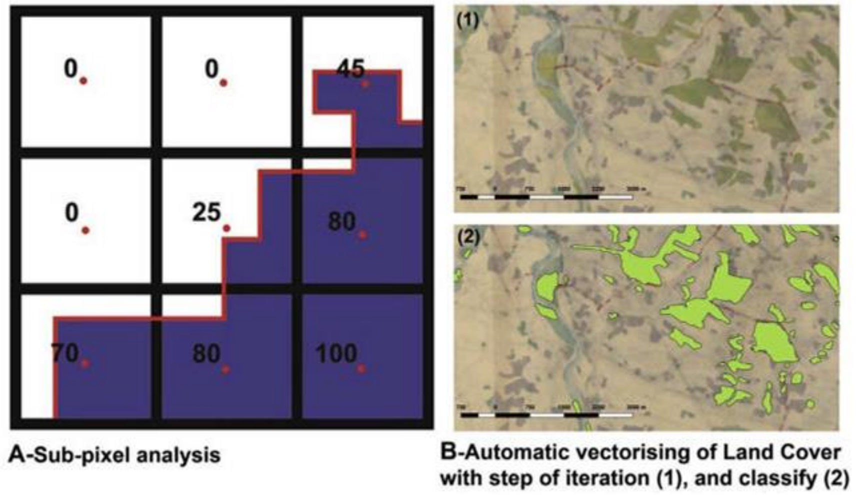

Fig. 3. A-Process of pixel and sub-pixel analysis with percent of phenomena and marked borders; B-Automatic process of vectorizing raster data from the printed topographic maps by (1) iteration and (2) classification.

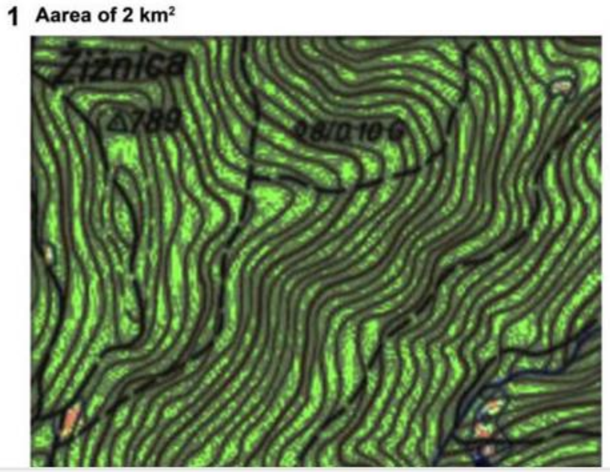

of pixels (points) representing a tree at a particular scale and in a proposed unit of 1 ha (Fig. 4).

The process of vectorisation follows the process of pixelisation. The process of scattered pixels in an area provides later manipulation in GIS software QGIS and SAGA for obtaining density and the number of trees. Although there are a few other methods, priority is given to ordinary kriging and global kriging methods. These methods include autocorrelation or the statistical relationship among the measured points and are very flexible in the presentation of forest distribution and density (Malczewski, 2004; Pew & Larsen, 2001). Data on the felled trees were obtained in comparison with TMs, new remote sensing data, and also from the official data from "National Serbia Woods" and "Šik Kopaonik" enterprises.

Finally, for estimating the total number of trees more precisely, we used other data such as cadaster books, census data, and strategic documents of the Republic of Serbia.

Applied Geography 92 (2018) 131–139

Contents lists available at ScienceDirect

Applied Geography

journal homepage: www.elsevier.com/locate/apgeog

GIS numerical and remote sensing analyses of forest changes in the Toplica region for the period of 1953–2013

Aleksandar Valjarević[a,b,*], Tatjana Djekić[c], Vladica Stevanović[d], Radomir Ivanović[d], Bojana Jandziković[d]

[a] Department for Management of Science and Technology Development, Ton Duc Thang University, Ho Chi Minh City, Viet Nam
[b] Faculty of Environment and Labour Safety, Ton Duc Thang University, Ho Chi Minh City, Viet Nam
[c] University of Niš, Faculty of Science and Mathematics, Department of Geography, Višegradska 33, Niš, Serbia
[d] University of Kosovska Mitrovica, Faculty of Science and Mathematics, Department of Mathematics, Department of Geography, Lole Ribara 29, 38220, Kosovska Mitrovica, Serbia

A R T I C L E I N F O

Keywords:
Forest density
Forest distribution
GIS analysis
Remote sensing
Forest changes
Cadaster data
Republic of Serbia

A B S T R A C T

Although the Toplica region is situated in a forest-rich part of the Republic of Serbia, the region's four municipalities are not equally forested. Forests are an important resource for economic activities and the existence of flora and fauna, both globally and in the Republic of Serbia. Many initiatives around the world intend to protect and renew forest belts under the sponsorship of developed and developing countries (e.g. China, India, Russia, Brazil, or the G7). In this study, we reconstructed the condition of forests in the Toplica region over the last 60 years using remote sensing, topographic maps, geographical information system (GIS) analysis, and official data from cadaster books and censuses. In addition to changes in forested land, concurrent socio-economic changes have affected the distribution and density of forests. The total number of trees in the Toplica region in 2013 was determined by applying numerical GIS analyses to remote sensing data. We also reconstructed the state of forests in 1953 and used this to determine the total number of trees cut down within this period, as well as the forested

The pixel and swaping pixel methods

DE GRUYTER
Open Astron. 2019; 28: 85–94

Research Article

Aleksandar Valjarević*, Dragica Živković, Nebojša Gadžić, Dušan Tomanović, and Mirko Grbić

Multi-criteria GIS analysis of the topography of the Moon and better solutions for potential landing

https://doi.org/10.1515/astro-2019-0008
Received Feb 15, 2019; accepted Mar 15, 2019

Abstract: During the past twenty years, the need to reach the Moon by the private space missions has been growing. Some of the private missions are supported by Google Lunar X-prize and Space-X. In the period between 2020 and 2050 private companies will be planning landing to the Moon with their own capacity. These missions can send new geodesy and cartography data. Lunar topography modelling with new satellite and remote sensing data gives plenty of possibilities for its exploration. GIS (Geographical Information System) may be successfully to the Moon topography analysis. According ... racteristics for landing.
... nd 3,000 m and on the
... n of 3° and azimuth of
... graphy and relief. With
... ial mission to the Moon

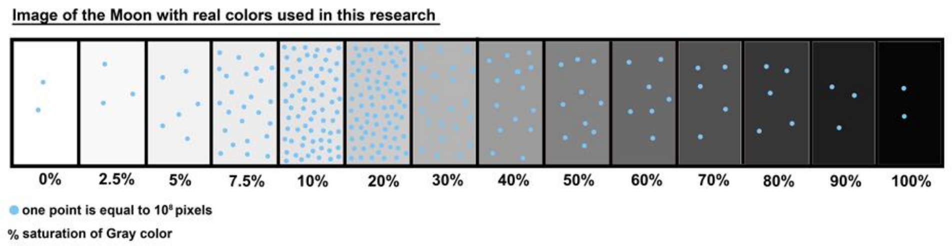

Figure 3. Moon recordings after total analysis in GIS, blue spots present shade with elevation more than 3000 m, grey scale colors were used to determine relief and surface of the Moon.

$$G = \ln 256 \times \ln 2 \times \sqrt{256} \quad (5)$$

This equation must be presented in short form:

$$G = ln158 \times \frac{\sqrt{256}}{2} =\sim 5 \times 16/2 =\sim 40 \quad (6)$$

Final equation, sustainable for each gray scale pixels is:

$$\lambda_{ij} = exp\left(\frac{-h_{ij}}{a}\right) \times 40 const. \quad (7)$$

4.2 GIS analysis and distribution of craters on the Moon

In the earlier stages of the manuscript, we explained how we determined the number and distribution of the craters.

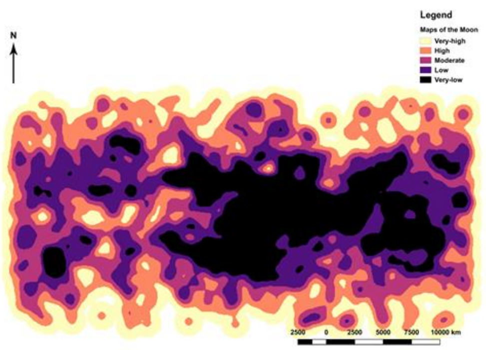

Figure 4. Distribution of Topography of the Moon, divided into 5 classes after GIS analyses.

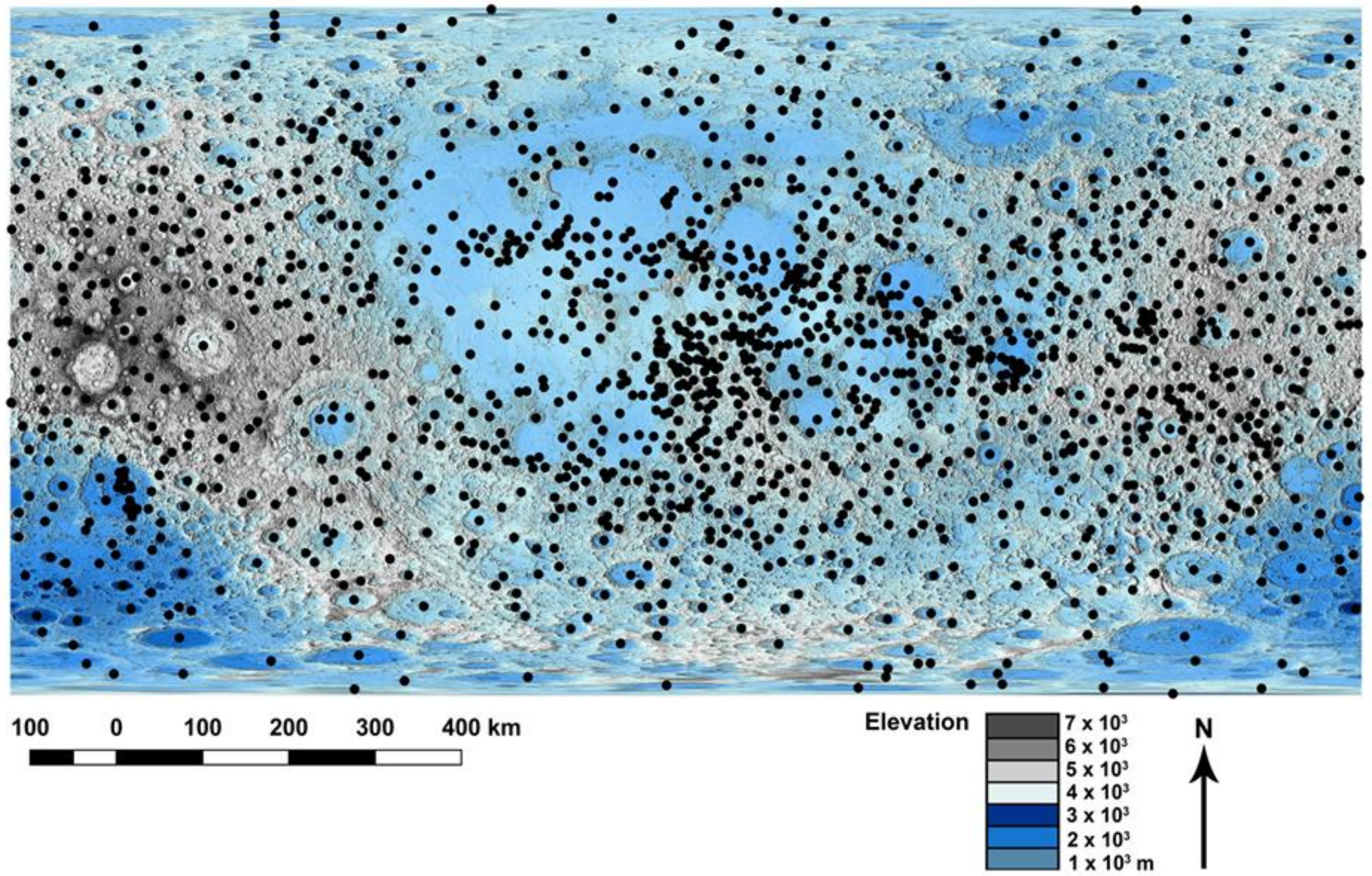

Figure 1. Map of the Moon with distribution of main craters longer than 300 m diameter

Results

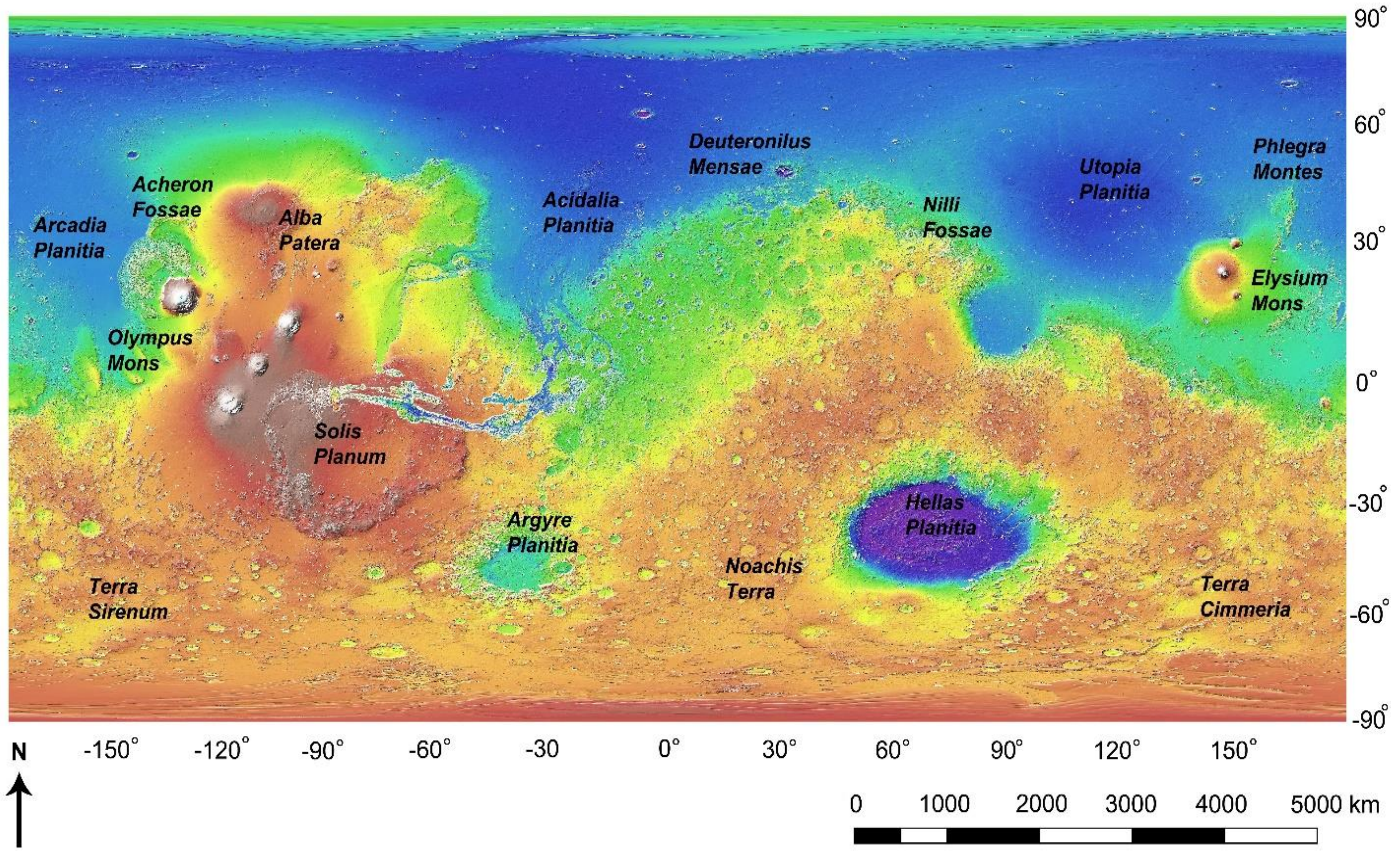

The data from the Mars missions were analyzed, evaluated and georeferenced. Two types of data were also used: Vector and raster data. The first map that was analyzed has a resolution of 1 km^2. The main Martian formations were identified and then these locations are analyzed and compared with the winds (dune formations).

Results

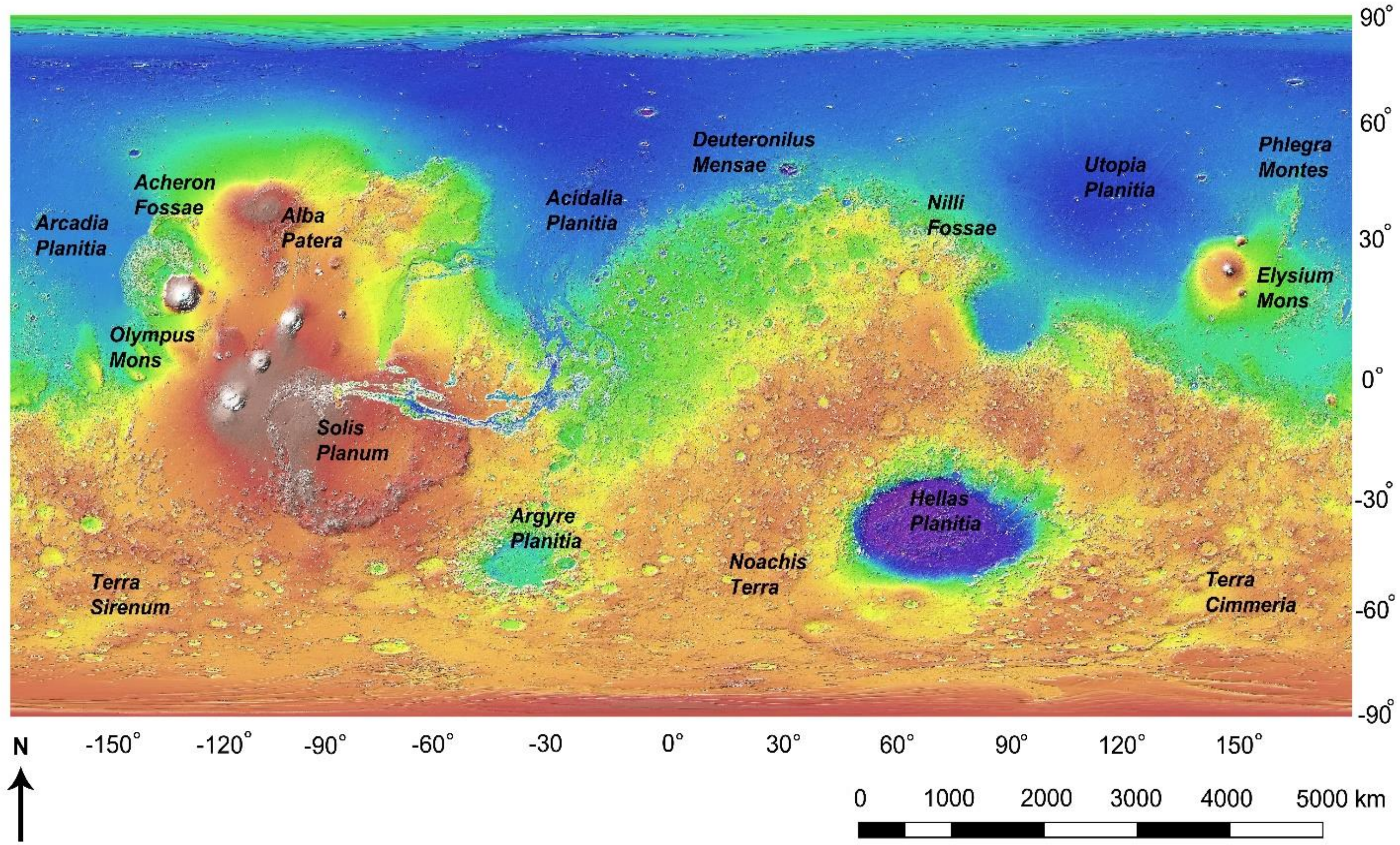

A detailed map of the dunes was created using data from Planet 2 and all satellite images from the last twenty years. The resolution of the dunes is 1 km^2.
Apart from the data of the dune shapes, which are estimated in meters (m), the other satisfactory data are the azimuth of the dune tracks, the center of gravity of the dune field, the average slip area and the azimuth points.

Results

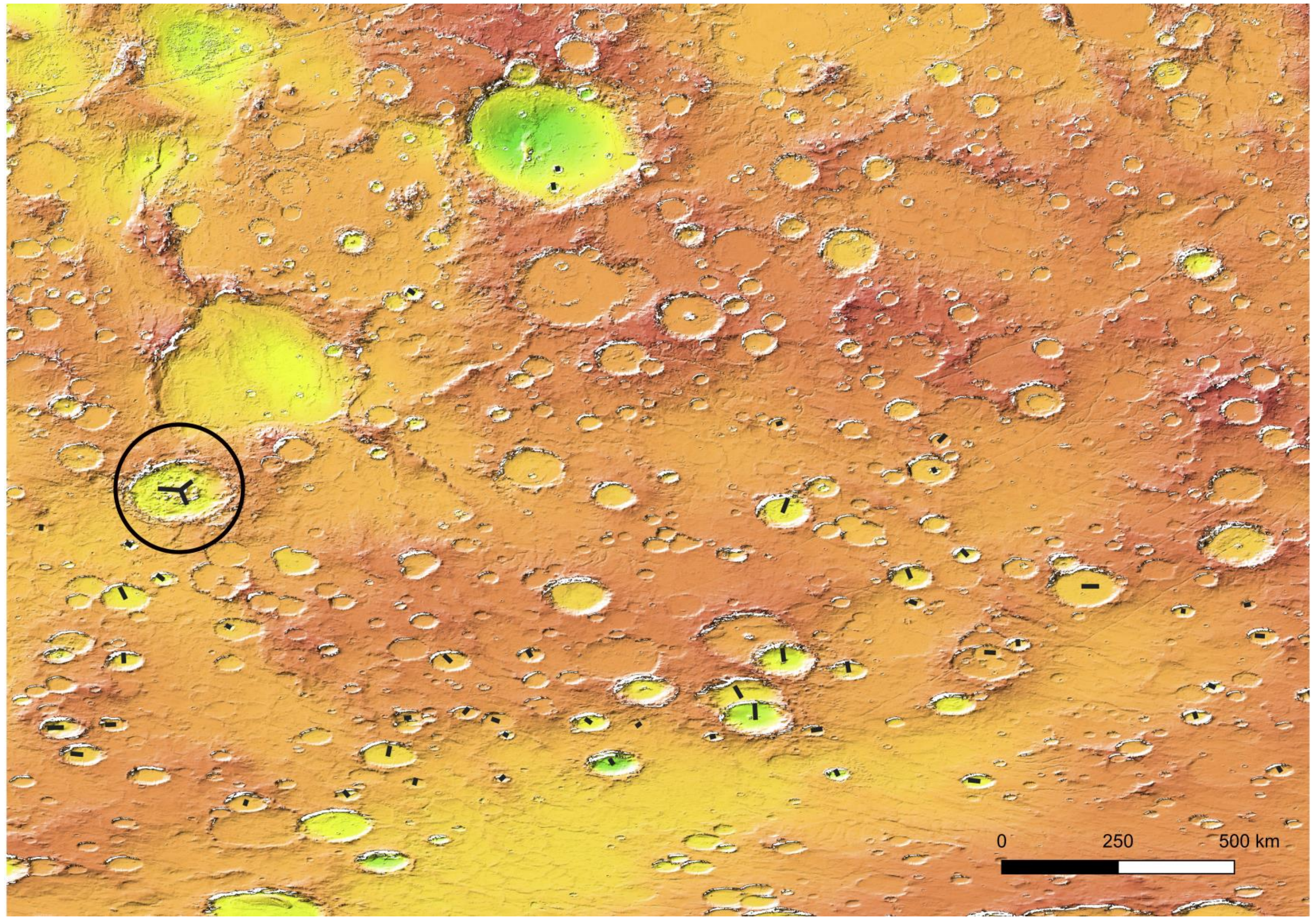

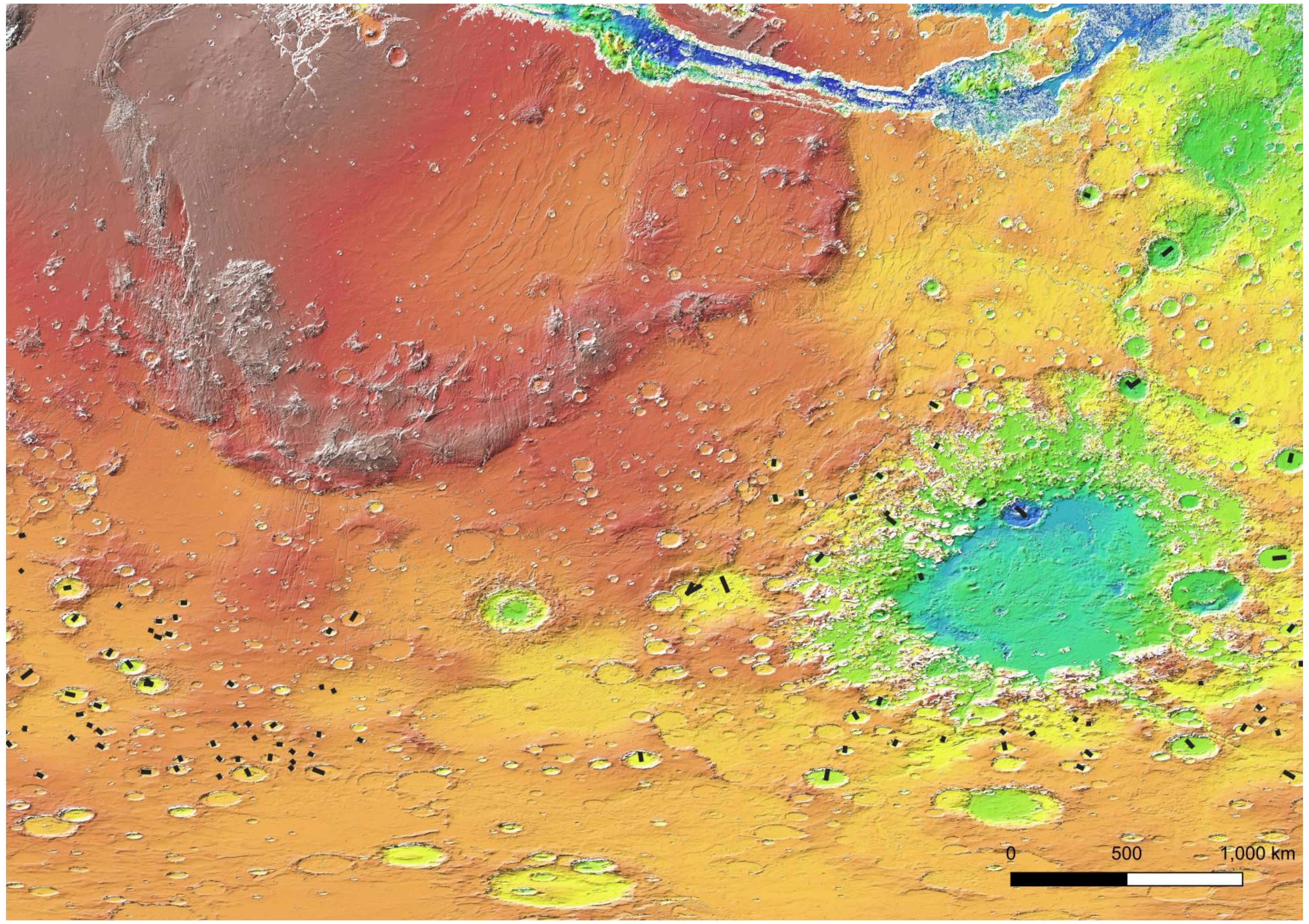

The analyses of the dune shapes are important to better understand the winds of the past on Mars. Two main types of dunes have been found on the planet Mars, stellar and linear dunes.

Results

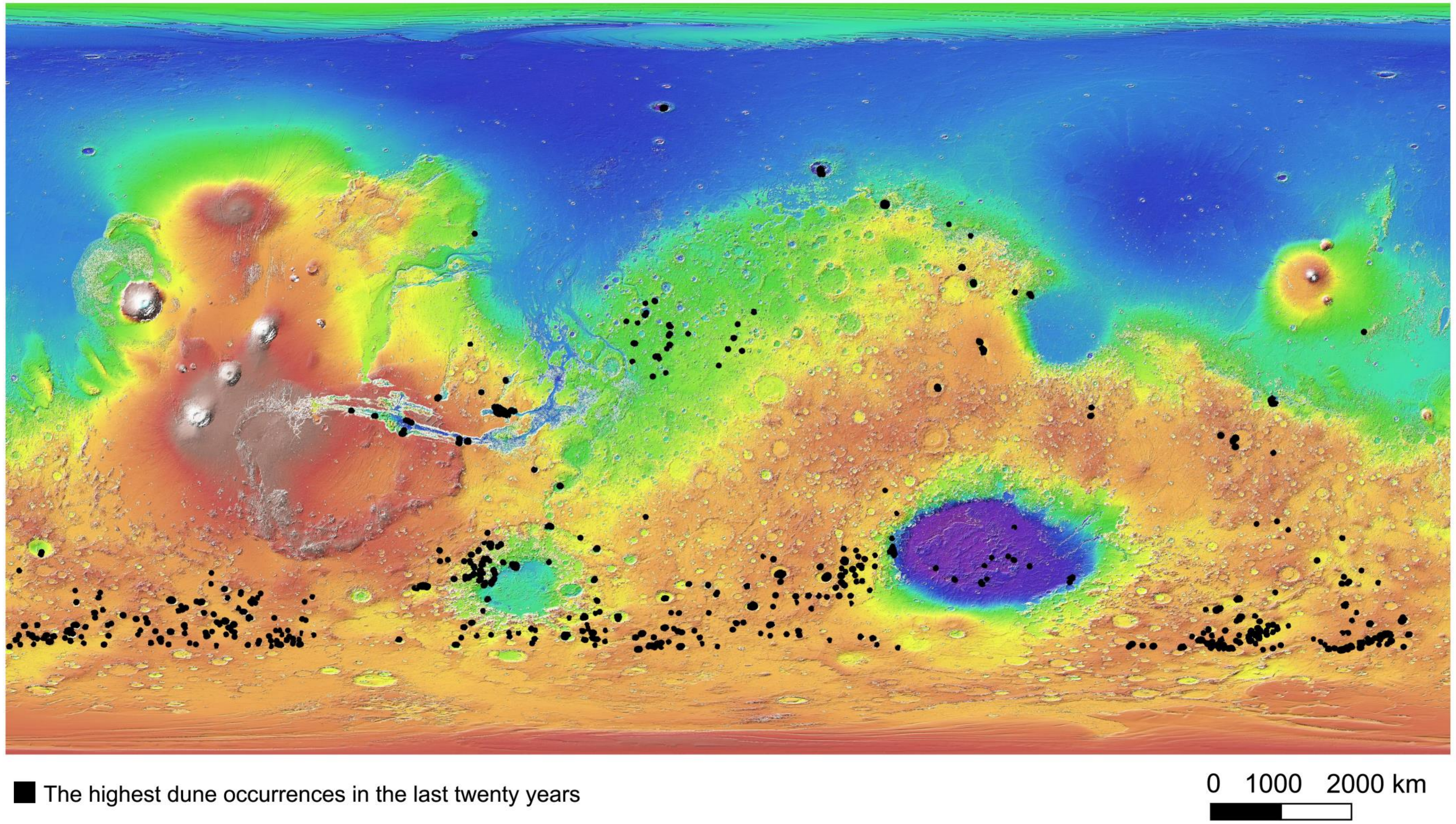

The concetration of all dunes on the planet Mars

Results

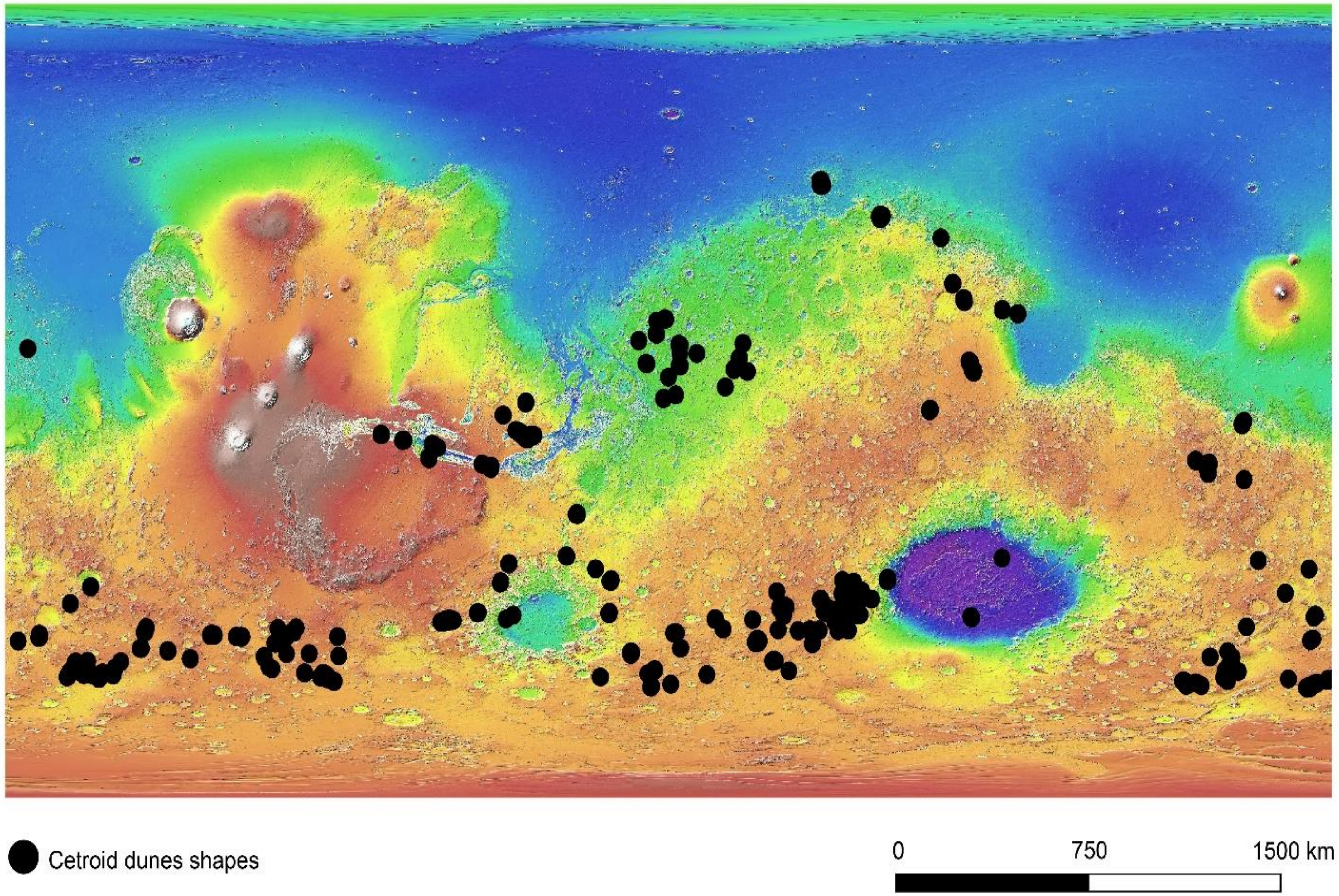

In the period (2000-2020) the dune tracks in the south-west were between -90° W and -180° W and -30° S and -70° S. The longest dune belt was in the *Terra Sirenum* belt, the total area of all dune tracks is 3117 km^2. The longest dune tracks for the period (2000-2020) are in the far west at 458.5 km. The isolated dunes have a maximum area of 899.5 km^2 and a length of 333 km. According to satellite records, the dune tracks in this region ran through smooth plains of Aeolian deposits and eroded margins of pyroclastic series material.

The total area of all dunes in this area is 584.5 km^2. The longest dune track is 115 km long. The dune tracks run through the smooth plains consisting of aeolian deposits. Aeolian erosion is most pronounced in this region due to the sandy subsoil. The third dune belt is the second largest in terms of area. The total area of this belt is 2897 km^2 with a longest stretch of 390 km, from west to east. Compared to the first dune belt, the winds blow from west to east. In the first dune belt, the winds blow from north to south

Results

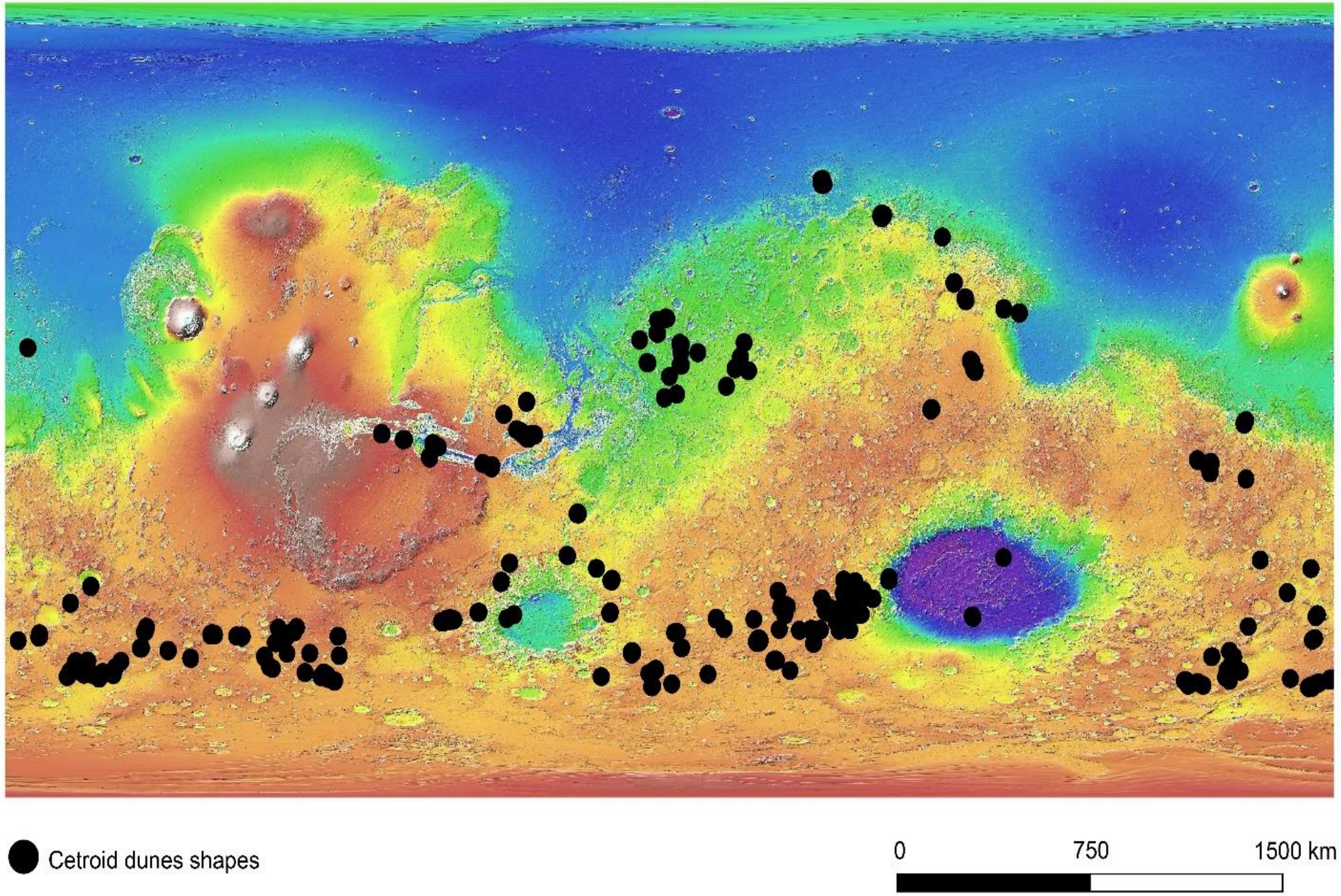

The fourth and fifth belts, are very small belta and located in the Promethei Terra region. This dune belt has an area of 70 km^2 and the longest trajectory is 24 km. The fifth belt has an area of 1799 km^2 and the longest trajectory is 245 km. This belt is located in the Terra Cimmeria region and consists of pyroclastic series material and hilly lava plains. The winds blow from north to south. This belt has geographical coordinates of +90°E and -30°S.

The sixth dune belt is located in the region between Terra Cimmeria in the south and Elysium Mons. The area of this belt is 2120 km^2 with a longest path of 145 km. The geology of this region varies between hilly lava plains, pyroclastic series material and aeolian deposits. The seventh belt is located near the Arabia Terra region. This belt has an area of 1340 km^2 with the longest stretch of 175 km, from north to south. This belt has the geographical coordinates +60°E and +45°N. The eighth dune belt is located between the Arabia Terra and Terra Meridani regions and very close to the Martian equator. The total area is 1560 km^2 with a longest stretch of 145 km. The geology of this region consists of hilly lava plains, pyroclastic series material, eolian deposits and plains with lava channels.

Results

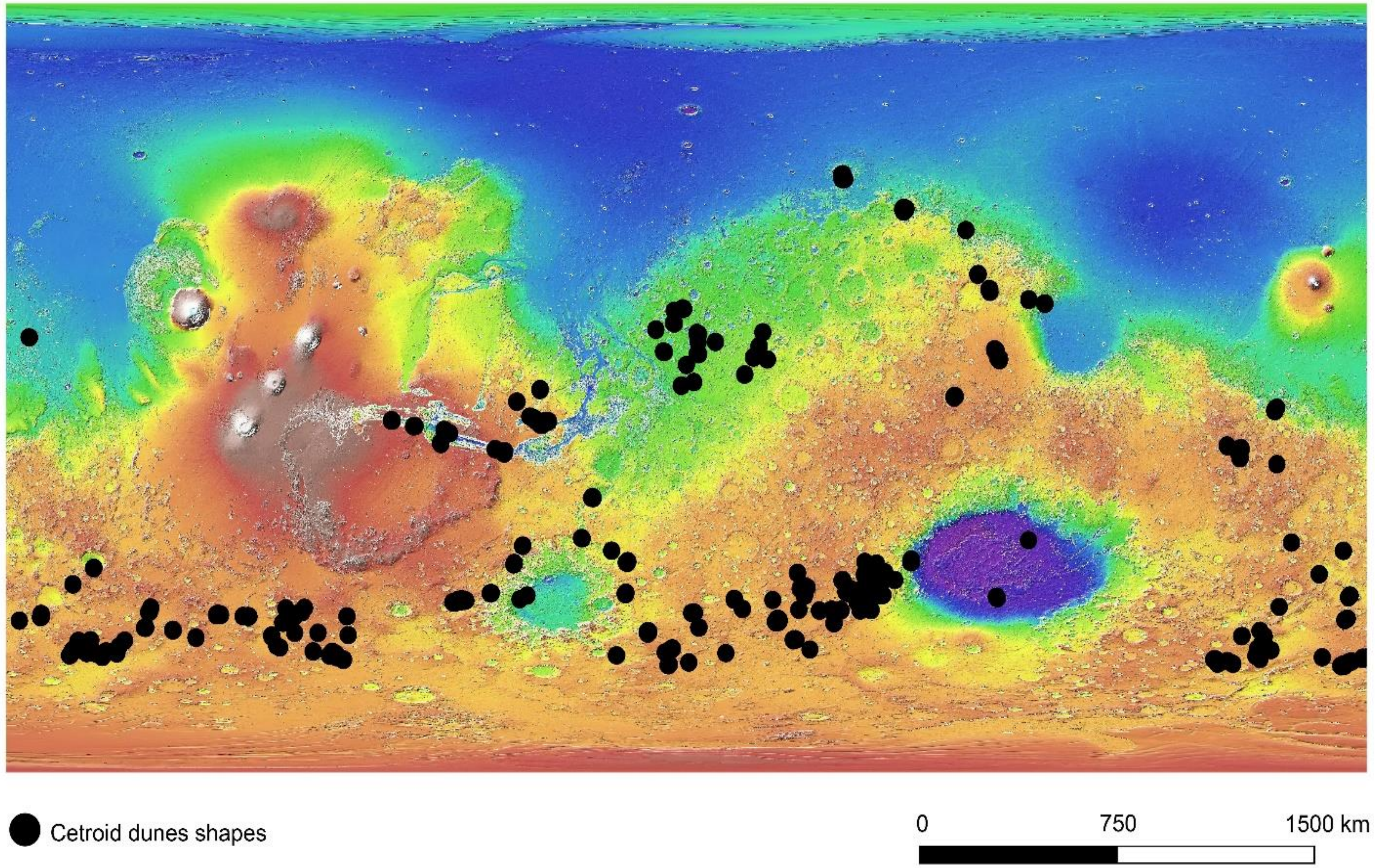

The tenth dune belt is the most isolated and very small in area. The area is 60 km^2 and the longest path is 22 km long. The coordinates of this region are -170°E and +20°N. This belt consists of pyroclastic series material, Aeolian deposits. This belt is located 450 km to the east, far from the highest point of the planet Mars, Olympus Mons (21,900 m).

The high acceleration has dunes in the first, second and third belts. The azimuth of the dunes in the first belt between -120°E and -30°S showed that most of the azimuths were in the direction of –80°S and -90°S.

Systematic GIS analysis revealed 10 (ten) dune belts dependent on satellite imagery over the last twenty years. Most occurrences of dune activity are measured in the left quadrant between -150°E and -90°E and -40°S and +10°S. The sum of all dune areas is 14,297 km^2 and accounts for 0.009% of the area of the planet Mars. The sum of all dune paths over the last twenty years is 2038.5 km and corresponds to 60% of the length of the equator on the planet. The geological background compared with the dune tracks showed that in 70% of cases the dunes had to move on Aeolian deposits, in 20% on pyroclastic series material and in 10% on other geological layers. Based on the downloaded vector data and the comparison with the satellite records for Planet, the azimuth of all dune tracks was estimated. The Planet 2 and USGS data helped with the accuracy of the analyzed data.

Conlusions

The tenth belt consists of 80 % Aeolian deposits and 20 % rugged lava plains. The trajectories of the dunes in this belt have an azimuth between -90°W and -30°W. For this reason, all winds in this belt typically have a westerly direction. The dunes in this belt only follow the westerly direction on the planet Mars. The winds in the past of the planet Mars showed greater activity in the past, especially from 200,000,000 years ago. The dunes of the south meridians and their frequencies have slowed down in the last 80,000 years. In recent times, the winds are very rare and the dune activity is no longer present.

This planet could be a habitable planet and analyzing the relief features is of enormous importance for humanity. This analysis provided some new insights into the course of the dunes in the geological past by comparing different geological units. Geographic Information Systems (GIS) and numerical analyses can contribute to a better understanding of Martian soils, features and geomorphological structures. The ten Martian soil belts are subdivided into dune processes, geological and geomorphological features. All belts are independent of each other and have very specific features and structures on the planet Mars. The planet Mars was analyzed structurally and at different spatial angles in this study. The long-term analyses (2010-2020) of the ten-year satellite images are good for a better view of the structures of the planet's surface. This research can be expanded in the future with the new satellite images with better spatial resolutions. This research is also important because it shows the activity of the Martian atmosphere in the past and in recent times. The winds on the planet Mars are important for the aeolian processes. A further significance lies in the proof that Mars had a deeper atmosphere in the geological past.

Tharsis Region the region with most active large dunes in the past

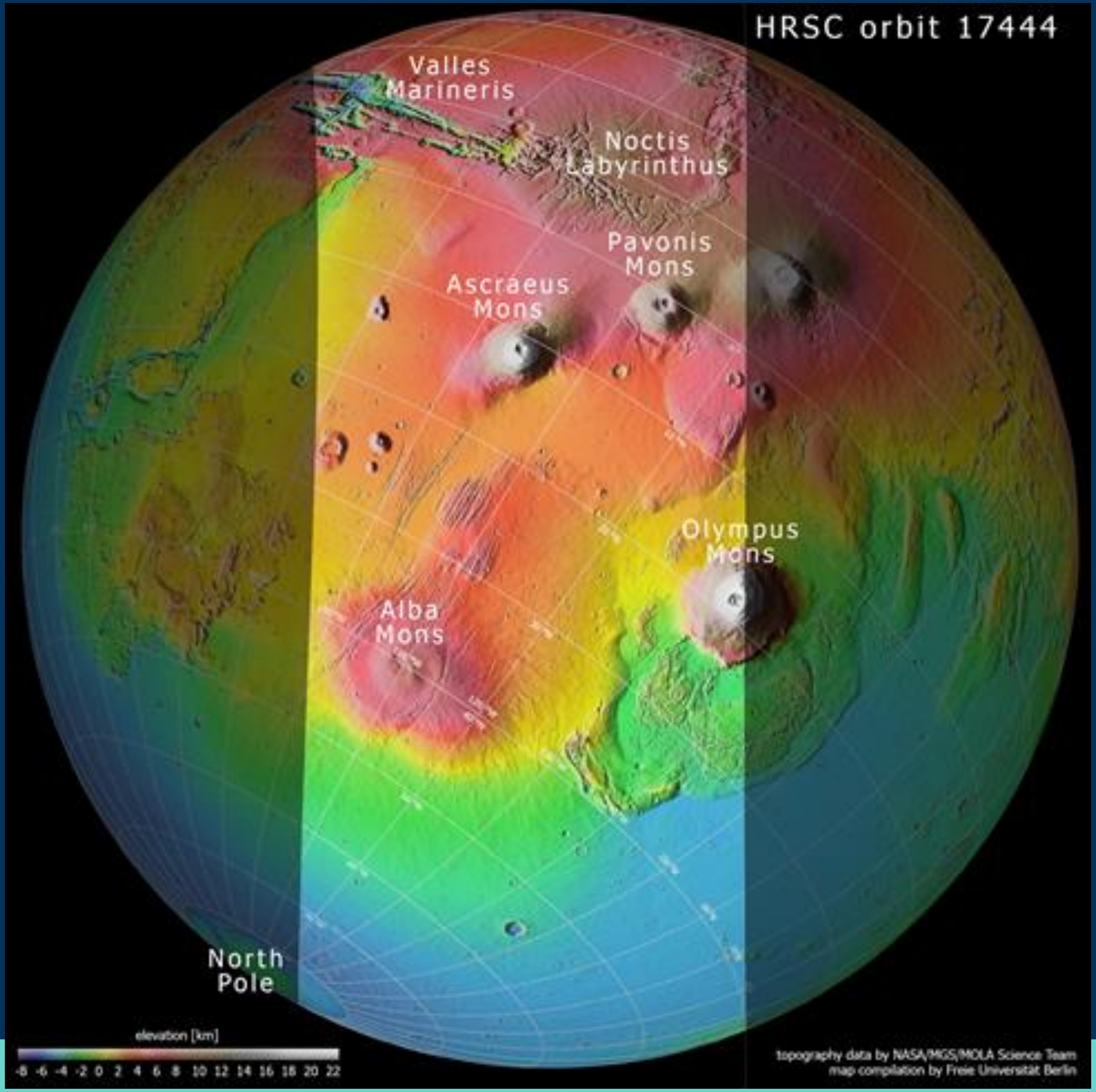

Leading papers

- Valjarević, A., Djekić, T., Stevanović, V., Ivanović, R., & Jandziković, B. (2018). GIS numerical and remote sensing analyses of forest changes in the Toplica region for the period of 1953–2013. *Applied geography*, 92, 131-139.
- Valjarević, A., Srećković-Batoćanin, D., Valjarević, D., & Matović, V. (2018). A GIS-based method for analysis of a better utilization of thermal-mineral springs in the municipality of Kursumlija (Serbia). *Renewable and Sustainable Energy Reviews*, *92*, 948-957.
- Valjarević, A., Filipović, D., Valjarević, D., Milanović, M., Milošević, S., Živić, N., & Lukić, T. (2020). GIS and remote sensing techniques for the estimation of dew volume in the Republic of Serbia. Meteorological Applications, 27(3), e1930.
- Valjarević, A., Popovici, C., Štilić, A., & Radojković, M. (2022). Cloudiness and water from cloud seeding in connection with plants distribution in the Republic of Moldova. Applied Water Science, 12(12), 262.
- Valjarević, A., Milanović, M., Gultepe, I., Filipović, D., & Lukić, T. (2022). Updated Trewartha climate classification with four climate change scenarios. *The Geographical Journal*, *188*(4), 506-517.

Leading papers

Valjarević, A., Algarni, S., Morar, C., Grama, V., Stupariu, M., Tiba, A., & Lukić, T. (2023). The coastal fog and ecological balance for plants in the Jizan region, Saudi Arabia. *Saudi Journal of Biological Sciences*, *30*(1), 103494.

Valjarević, A., Popovici, C., Djekić, T., Morar, C., Filipović, D., & Lukić, T. (2022). Long-term monitoring of high optical imagery of the stratospheric clouds and their properties new approaches and conclusions. *The Egyptian Journal of Remote Sensing and Space Science, 25(4), 1037-1043.88*(4), 506-517.

Gulan, L., Valjarevic, A., Milenkovic, B. et al. Environmental radioactivity with respect to geology of some Serbian spas. J Radioanal Nucl Chem 317, 571–578 (2018). https://doi.org/10.1007/s10967-018-5914-1

Valjarević, A., Živković, D., Gadžić, N., Tomanović, D., & Grbić, M. (2019). Multi-criteria GIS analysis of the topography of the Moon and better solutions for potential landing. *Open Astronomy*, *28*(1), 85-94.

Taofeek O. M. …….Valjarević, A........... (2024). Global analyses of the savannah with the included climate change effects. Science (in accepatnce).

Valjarević et al., (2024). GIS-based methods and analyses of past dunes and wind paths on the planet Mars based on satellite images from 2010-2020. Submited to the Serbian Astronomical Journal.